INSTITUTE FOR FUSION STUDIES

DOE/ET-53088-561 IFSR #561

The Electrostatic Wake of a Superthermal Test Electron in a Magnetized Plasma

A.A. WARE
Institute for Fusion Studies
The University of Texas at Austin
Austin, Texas 78712
and
J.C. WILEY
Fusion Research Center
The University of Texas at Austin
Austin, Texas 78712

July 1992

THE UNIVERSITY OF TEXAS

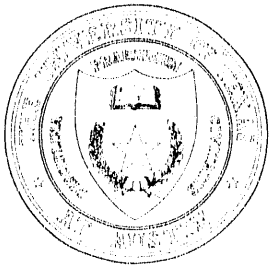

AUSTIN

The Electrostatic Wake of a Superthermal Test Electron in a Magnetized Plasma

A.A. Ware
Institute for Fusion Studies
The University of Texas at Austin
Austin, Texas 78712
and
J.C. Wiley
Fusion Research Center
The University of Texas at Austin
Austin, Texas 78712

DOE/ET/53088--561

DE92 019394

Abstract

The electrostatic potential is determined for a test electron with $v_{||} \gg v_{Te}$ in a uniform magnetized plasma ($\omega_{ce} \gg \omega_{pe}$). In the frame of the test electron, part of the spatially oscillatory potential has spherical symmetry over the hemisphere to the rear of the electron and is zero ahead of the electron. A second part of different character, which makes the potential continuous at the plane containing the electron, is oscillatory in the radial direction but decreases almost monotonically in the axial direction.

I. Introduction

There is evidence that electrons with $v_{\|} \gtrsim v_{Te}$ in a magnetized plasma interact strongly with each other. Thus the energetic electron tail observed flowing parallel to the electron current at the edge of reversed field pinches[1] presents evidence not only of strong transport of parallel momentum and energy from more central parts of the plasma but of strong mutual interaction. The evidence for strong interaction is that these electrons have a distribution in $v_{\|}$ which is a half-Maxwellian, the effective $T_{\|}$ being more than an order of magnitude larger than the T_e for the bulk electrons. In completely unrelated numerical particle simulations[2] there is similar evidence. To a magnetized plasma of Maxwellian electrons and ions a current of test electrons was added with constant distribution from v_{Te} to $6v_{Te}$. In a time for the electron-ion collisions to reduce the current by 16%, there being no applied electric field, the background electrons flowing parallel to the electron current and the test electrons had relaxed to a half-Maxwellian, the effective temperature being substantially higher than the unchanged temperature of the background electrons flowing in the reverse direction. Strong transport of parallel momentum and energy was observed but negligible particle transport. There was no magnetic turbulence and because of the two-dimensional character of the simulation no electrostatic particle transport. An enhanced level of electron plasma waves was observed and Decyk *et al.* identified these waves as the cause of the observed transport and the strong interactions. As a first step in understanding the interaction of such electrons and their wave emission this paper is concerned with determining the electrostatic wake field of such electrons.

The reaction of a uniform plasma to the electrostatic field of a moving test electron was studied by Rostoker and Rosenbluth[3] for the two cases with and without a uniform magnetic field. (This work is described in greater detail and clarity in a General Atomic Report.[4])

For a test electron having the velocity $v_0 \gg v_{Te}$ in the positive z-direction, the dielectric function for no magnetic field gives a resonance $k_z = \omega_{pe}/v_0$. As a result the emission of electron plasma waves by the test electron with given k is concentrated on the cone forming an angle θ with respect to $\mathbf{v}_0$, where $\cos\theta = k_z/k$. As shown by Rostoker and Rosenbluth, this leads to a Cerenkov-type shock front making the acute angle $\pi/2 - \theta$ with the negative z-axis. Their treatment of the case with a magnetic field was very general and involved no assumption concerning the relative magnitudes of ω_{pe} and ω_{ce}, the electron's plasma and cyclotron frequencies. The wake field was not determined for any specific case. They were aware that for the case $\omega_{ce} \gg \omega_{pe}$, where the field electrons in lowest order can respond to the waves only in the direction of $\mathbf{B}$, the resonance caused by the dielectric function has the different form $k = \omega_{pe}/v_0$, being independent of the direction of $\mathbf{k}$. The electron plasma waves involved in this case are the oblique plasma waves having the approximate dispersion relation $\omega_k = k_\parallel \omega_{pe}/k$. The different wake field that would result in this case was not studied.

Here, the electrostatic potential field is determined for such a magnetized plasma in the frame of reference moving with the test electron and it is the steady-state field ($t \to \infty$) which is of interest. It must be noted that O'Neil[5] showed that the linear Landau damping, which is an important part of the dielectric function, is not correct for long times. For the case of a wave packet, which is the case for a test electron, Landau damping can still be valid if the group velocity of the wave packet is different from the velocity of the resonant electrons.[6] But for a uniform magnetic field the group velocity of the test electron's wave packet in the direction of $\mathbf{B}$ is the same as the velocity of the test electron and the resonant electrons. However, it will be shown in an accompanying paper[7] that if a small amount of magnetic shear is present and because of the symmetry of the wake field the normal Landau damping is recaptured.

II. The Response of the Plasma to the Test Electron

A uniform plasma is considered in the presence of a uniform magnetic field (**B**) which is assumed sufficiently large so that $\omega_{ce} \gg \omega_{pe}$ and $\rho_e \ll \lambda_D$, where ρ_e is the electron Larmor radius and λ_D is the electron Debye length $v_{Te}/\sqrt{2}\,\omega_{pe}$, with $v_{Te}^2 = 2T_e/m_e$. Because of this assumption the perpendicular cyclotron motion of the test and field electrons is neglected. The test electron's velocity parallel to **B** is taken as v_0 with $v_0 \gg v_{Te}$. Also, due to the high frequencies involved, the very weak response of the ions is neglected and the equations to be solved for the perturbation to the electron distribution function, δf, and the potential Φ, are

$$\frac{\partial}{\partial t}(\delta f) + v_0\,\mathbf{i}_{\|}\cdot\nabla\delta f = \frac{q}{m}\,\mathbf{i}_{\|}\cdot\nabla\Phi\,\frac{\partial f_0}{\partial v_{\|}} \tag{1}$$

$$-\nabla^2\Phi = 4\pi q\,\delta(\mathbf{r}-\mathbf{r}_0-\mathbf{v}_0 t) + 4\pi q\int \delta f\, d^3v\ , \tag{2}$$

where $\mathbf{i}_{\|}$ is the unit vector parallel to **B**, f_0 is the unperturbed electron distribution function which is taken to be uniform and Maxwellian and q is used to denote the electron's charge to avoid unnecessary confusion with the minus sign ($q = -e$). The procedure for solving Eqs. (1) and (2) using Fourier and Laplace transforms can be found in Ref. 2 or in the textbook by Krall and Trivelpiece.[8] Choosing a reference frame moving with the test electron with the test electron at the origin and the z-axis parallel to **B**, the potential for $t \to \infty$ is given by

$$\Phi(\mathbf{r}) = \frac{4\pi q}{(2\pi)^3}\int d^3k\left[\frac{\lambda_D^2\, e^{i\mathbf{k}\cdot\mathbf{r}}}{k^2\lambda_D^2 - W_R + i\,W_I(k_{\|}/|k_{\|}|)}\right]\ , \tag{3}$$

where

$$-W_R + i\,W_I\left(\frac{k_{\|}}{|k_{\|}|}\right) = z\,Z(z) + 1 \tag{4}$$

$$z = \frac{k_{\|}}{|k_{\|}|}\,\frac{v_0}{v_{Te}} \tag{5}$$

and Z is the plasma dispersion function. For $v_0 \ll v_{Te}$,

$$W_R \simeq \frac{v_{Te}^2}{2v_0^2} , \qquad W_I = \pi^{1/2} \frac{v_0}{v_{Te}} \ell^{-\frac{v_0^2}{v_{Te}^2}} . \tag{6}$$

III. The Fourier Inversion Integrals

In order to put Eq. (3) in dimensionless form, the substitutions $\kappa = k\lambda_D$, $\hat{r} = r/\lambda_D$ are made. Then with cylindrical coordinates in k-space, namely $k_\perp, \phi, k_z$ and cylindrical coordinates in real space, r, θ, z the potential is given by

$$\hat{\Phi} \equiv \frac{\Phi\lambda_D}{q} = \frac{1}{2\pi^2} \int_0^\infty \kappa_\perp \, d\kappa_\perp \int_0^{2\pi} d\varphi \, e^{i\kappa_\perp \hat{r}\cos\phi} \int_{-\infty}^{+\infty} d\kappa_z \, e^{i\kappa_z \hat{z}} \left\{ \frac{1}{(\kappa_z^2 - W_R + \kappa_\perp^2 + iW_I)} \right|_{\kappa_z > 0}$$

$$+ \left. \frac{1}{(\kappa_z^2 - W_R + \kappa_\perp^2 - iW_I)} \right|_{\kappa_z < 0} \Bigg\} . \tag{7}$$

Making the substitutions

$$\alpha_+ = \alpha + i\beta , \qquad \alpha_- = \alpha - i\beta , \qquad \text{with} \qquad (\alpha + i\beta)^2 = W_R - \kappa_\perp^2 + i\, W_I , \tag{8}$$

where α and β are real and positive, the κ_z-integral in Eq. (7) can be written in the form

$$I = \int_0^\infty d\kappa_z \Bigg\{ \cos(\kappa_z|\hat{z}|) \left[\frac{1}{\kappa_z^2 - \alpha_-^2} + \frac{1}{\kappa_z^2 - \alpha_+^2} \right]$$

$$\pm \; i\sin(\kappa_z|\hat{z}|) \left[\frac{\kappa_z}{\alpha_-(\kappa_z^2 - \alpha_-^2)} - \frac{\kappa_z}{\alpha_+(\kappa_z^2 - \alpha_+^2)} - \frac{1}{\alpha_-(\kappa_z + \alpha_-)} + \frac{1}{\alpha_+(\kappa_z + \alpha_+)} \right] \Bigg\} . \tag{9}$$

The positive sign preceding the sine term applies for $z > 0$, the negative sign for $z < 0$. The cosine part and the first two terms in the sine part can be converted to standard contour

integrals and the remaining two sine terms are in a standard form. The result is

$$I_{z>0} = i\left[\frac{f(\alpha_+|\hat{z}|)}{\alpha_+} - \frac{f(\alpha_-|\hat{z}|)}{\alpha_-}\right]$$

$$I_{z>0} = i\pi\left[\frac{e^{i\alpha_+|\hat{z}|}}{\alpha_+} - \frac{e^{-i\alpha_-|\hat{z}|}}{\alpha_-}\right] - I_{z>0} \tag{10}$$

where f is the auxiliary sine integral defined by

$$f(z) = Ci(z)\sin z + \left[\frac{\pi}{2} - Si(z)\right]\cos z\ .$$

Substituting from Eq. (10) into Eq. (7), noting that the ϕ-integral gives $2\pi J_0(\kappa_\perp \hat{r})$ the potential fore and aft of the test electron is given by

$$\hat{\Phi}_{z>0} = \hat{\Phi}_1 = \frac{i}{\pi}\int_0^\infty \kappa_\perp\, d\kappa_\perp\, J_0(\kappa_\perp \hat{r})\left[\frac{f(\alpha_+|\hat{z}|)}{\alpha_+} - \frac{f(\alpha_-|\hat{z}|)}{\alpha_-}\right] \tag{11}$$

$$\hat{\Phi}_{z<0} = -\hat{\Phi}_1 + \int_0^\infty \kappa_\perp\, d\kappa_\perp\, J_0(\kappa_\perp \hat{r})\left[\frac{e^{-(\kappa_\perp^2+\beta_+^2)^{1/2}|\hat{z}|}}{(\kappa_\perp^2+\beta_+^2)^{1/2}} + \frac{e^{-(\kappa_\perp^2+\beta_-^2)^{1/2}|\hat{z}|}}{(\kappa_\perp^2+\beta_-^2)^{1/2}}\right] \tag{12}$$

$$\text{where } \beta_+ = b + ia,\ \beta_- = b - ia \qquad \text{and} \qquad (a+ib)^2 = W_R + i\,W_I\ . \tag{13}$$

Making the substitution in both parts of the integral in Eq. (12)

$$y = \frac{(\kappa_\perp^2+\beta_\pm^2)^{1/2}}{\beta_\pm}$$

each part reduces to the known integral[9]

$$\beta_\pm \int_1^\infty dy\, e^{-\beta_\pm v|\hat{z}|}\, J_0\left[\beta_\pm \hat{r}(y^2-1)^{1/2}\right] = \frac{\beta_\pm\, e^{-(\beta_\pm^2\,\hat{z}^2+\beta_\pm^2\,\hat{r}^2)}}{(\beta_\pm^2\,\hat{z}^2+\beta_\pm^2\,\hat{r}^2)^{1/2}}$$

so that

$$\hat{\Phi}_{z<0} = \frac{2}{\hat{R}}\, e^{-b\hat{R}}\cos(a\hat{R}) - \hat{\Phi}_1 \tag{14}$$

where $\hat{R}$ is the distance from the test electron in units of $\lambda_D(\hat{R}^2 = \hat{r}^2 + \hat{z}^2)$.

IV. The Evaluation of $\widehat{\Phi}_1$

A. Limiting Cases

An analytic solution to the integral for $\hat{\Phi}_1$ in Eq. (11) has not been found. It has been necessary to resort to a computational method as described below. However, two limiting cases, namely $\hat{z} = 0$ and $\alpha_\pm|\hat{z}|$ large, have been solved and these help to illuminate the nature of this part of the potential.

Since $f(z)$ for $z = 0$ is $\pi/2$

$$\hat{\Phi}_1(\hat{z}=0) = \frac{i}{2}\int \kappa_\perp\, d\kappa_\perp\, J_0(\kappa_\perp \hat{r})\left(\frac{1}{\alpha_+} - \frac{1}{\alpha_-}\right)$$

$$= \frac{1}{2}\int \kappa_\perp\, d\kappa_\perp\, J_0(\kappa_\perp \hat{r})\left[\frac{1}{(\kappa_\perp^2+\beta_-^2)^{1/2}} + \frac{1}{(\kappa_\perp^2+\beta_+^2)^{1/2}}\right]$$

using Eqs. (8) and (13). This is again a standard integral (see Ref. 7, p. 682, number 6.554-1) giving

$$\hat{\Phi}_1(\hat{z}=0) = \frac{1}{2}\left(\frac{e^{-\beta_-\hat{r}}}{\hat{r}} + \frac{e^{-\beta_+\hat{r}}}{\hat{r}}\right) = \frac{e^{-b\hat{r}}}{\hat{r}}\cos a\hat{r}\,. \tag{15}$$

This result agrees with that which can now be obtained from Eq. (14) with $\hat{z} = 0$, so that the sum of two parts of the potential is continuous across the plane $z = 0$.

The asymptotic form of $f(z)$ for large z is z^{-1} and hence this potential for large $\hat{z}$ is

$$\hat{\Phi}_1(\hat{z}\to\infty) = \frac{i}{\pi|\hat{z}|}\int_0^\infty \kappa_\perp\, d\kappa_\perp\, J_0(\kappa_\perp\hat{r})\left(\frac{1}{\alpha_+^2} - \frac{1}{\alpha_-^2}\right)$$

$$= \frac{-i}{\pi|\hat{z}|}\int_0^\infty \kappa_\perp\, d\kappa_\perp\, J_0(\kappa_\perp\hat{r})\left[\frac{1}{\kappa_\perp^2+\beta_-^2} - \frac{1}{\kappa_\perp^2+\beta_+^2}\right]$$

$$= \frac{-i}{\pi|\hat{z}|}\left\{K_0[(b-ia)\hat{r}] - K_0[(b+ia)\hat{r}]\right\}$$

(Ref. 7, p. 678 number 6.532-4)

$$= \frac{1}{2|\hat{z}|}\left\{H_0^{(1)}[ib+a)\hat{r}] - H_0^{(1)}[(ib-a)\hat{r}]\right\}$$

$$= \frac{1}{2|\hat{z}|}\left\{H_0^{(1)}[(a+ib)\hat{r}] - H_0^{(2)}[(a-ib)\hat{r}]\right\} . \tag{16}$$

Here K_0 is the Bessel function of imaginary argument, $H_0^{(1)}, H_0^{(2)}$ are the Hankel functions of the first and second kind and the relationships $K_0(z) = (\pi i/2)H_0^{(1)}(iz)$, and $H_0^{(1)}(e^{i\pi}z) = -H_0^{(2)}(z)$ have been used.

B. Numerical Solution

$\hat{\Phi}_1$ can be written in terms of $g(z)$ where

$$g(z) = i\left[\frac{f(z)}{z} - \frac{f(z^*)}{z^*}\right] . \tag{17}$$

$g(z)$ is a real function as can be seen by explicitly expressing $g(z)$ in terms of real functions. Let $z = x + iy$, then

$$\begin{aligned} g(z) = {} & \frac{\pi}{x^2+y^2}\left[y\,\cos x\cosh y + x\,\sin x\,\sinh y\right] \\ & + \frac{2}{x^2+y^2}\Big[\left(y\,Ci^r(z) - x\,Ci^i(z)\right)\sin x\cosh y \\ & - \left(x\,Ci^r(z) + y\,Ci^i(z)\right)\cos x\,\sinh y \\ & - \left(y\,Si^r(z) - x\,Si^i(z)\right)\cos x\cosh y \\ & - \left(x\,Si^r(z) + y\,Si^i(z)\right)\sin x\,\sinh y\Big] \end{aligned}$$

where $Ci^r(z) = \text{Re}\ Ci(z)$, $Ci^i(z) = \text{Im}\ Ci(z)$ etc. For large z, g is given by

$$\begin{aligned} g(x+iy) \simeq 4\Bigg[& \frac{x\cdot y}{(x^2+y^2)^2} - 2!\,\frac{(2x^3y - 2xy^3)}{(x^2+y^2)^4} \\ & +4!\,\frac{(3x^5y - 10x^3y^3 + 3xy^5)}{(x^2+y^2)^6} - 8!\,\frac{(4x^7y - 28x^5y^3 + 28x^3y^5 - 4xy^7)}{(x^2+y^2)^8} + \cdots\Bigg] . \end{aligned} \tag{18}$$

$\hat{\Phi}_1$ can then be expressed in terms of g as

$$\hat{\Phi}_1 = \frac{1}{\pi}\int_0^\infty d\kappa_\perp\, J_0(\hat{r}\,\kappa_\perp)\kappa_\perp\,|\hat{z}|g\left(|\hat{z}|\sqrt{W_R - \kappa_\perp^2 + i\,W_i}\right)\ . \tag{19}$$

For large values of $\kappa_\perp$ the argument of g becomes approximately $i|\hat{z}|\kappa_\perp$. In this case g can be simplified by noting that

$$g(ix) = \pi\,\frac{e^{-x}}{x}\ .$$

Since

$$\int_0^\infty J_0(ax)e^{-bx}\,x dx = \frac{1}{(a^2+b^2)^{1/2}}\ ,$$

$\hat{\Phi}_1$ can be rewritten as

$$\hat{\Phi}_1 = \frac{1}{(\hat{r}^2+\hat{z}^2)^{1/2}} +$$

$$\frac{1}{\pi}\int_0^\infty \kappa_\perp\, d\kappa_\perp\, J_0(\hat{r}\,\kappa_\perp)\left\{|\hat{z}|g\left(|z|\sqrt{W_R - \kappa_\perp^2 + i\,W_I)}\right) - \frac{\pi}{\kappa_\perp}\,e^{-|\hat{z}|\kappa_\perp}\right\}\ . \tag{20}$$

The factor in braces goes to zero rapidly for $\kappa_\perp^2 \gg W_R$ allowing the numerical integration to be carried out over a modest range of $\kappa_\perp$.

The numerical quadrature was done using Mathematica.[10] Figure 1 shows $\hat{\Phi}_1$ as a function of $\hat{r}$ for $v_0/v_{Te} = 2.5$ (see Eq. (6)) and values of $\hat{z}, \{0.1, 1, 10, 100\}$. Note the scale change with increasing $\hat{z}$.

V. Summary and Discussion

Changing back from dimensionless units, the result obtained for the wake field of a superthermal test electron in the frame of reference moving with the test electron is

for $z > 0$,

$$\Phi(r,z) = \Phi_1 = -\frac{e}{\lambda_D}\,\hat{\Phi}_1 \tag{21}$$

for $z < 0$,

$$\Phi(r,z) = -\frac{2e}{R}\,\exp\left(-\frac{R}{\lambda_{\rm eff}}\right)\cos kR - \Phi_1 \tag{22}$$

where

$$R = (r^2 + z^2)^{1/2}\ ,$$

$$\lambda_{\rm eff} = \lambda_D/b = 2\lambda_D^2\,k/W_I\ ,$$

$$k = a/\lambda_D = \left[W_R + (W_R^2 + W_I^2)^{1/2}\right]^{1/2}/\sqrt{2}\,\lambda_D\ ,$$

where for a Maxwellian f_{e0} the values of W_R, W_I are given in terms of the plasma dispersion function by Eqs. (4) and (5). Equations (21) and (22) will still apply for non-Maxwellian f_{e0} when the appropriate values of W_R and W_I are used.

Examples of $\hat{\Phi}_1$ are shown in Fig. 1 and an example of the total $\hat{\Phi}$ for a given r is shown in Fig. 2. The limiting value of $\hat{\Phi}_1$ for $z \to 0$ gives

$$\Phi(r,0) = -\frac{e}{r}\,\exp\left(-\frac{r}{\lambda_{\rm eff}}\right)\cos kr \tag{23}$$

and from Eqs. (21) and (22) Φ is seen to be continuous across the plane $z = 0$. As z increases from zero the zeros and interlaced maxima and minima in $\hat{\Phi}_1(\hat{r})$ move to somewhat larger values of $\hat{r}$ and are seen to take up the places for a damped J_0 Bessel function (see comparison in Fig. 3). Apart from this moderate movement of the oscillations in $\hat{r}$, $\hat{\Phi}_1$ is oscillatory only in the r-direction and decreases monotonically in z.

Using the asymptotic approximation for the auxiliary sine integral for large argument, the approximate analytic solution for $\hat{\Phi}_1$ in Eq. (16) gives

$$\Phi_1(z \to \infty) = -\frac{e}{2z}\left\{H_0^{(1)}\left[(k + i\lambda_{\rm eff}^{-1})r\right] + H_0^{(2)}\left[(k - i\lambda_{\rm eff}^{-1})r\right]\right\} \tag{24}$$

where the H-symbols are the Hankel function. From the value of these functions at $r = 0$,

$$\Phi_1(0, z \to \infty) = -\frac{e}{z}\left[1 - \frac{2}{\pi}\tan^{-1}\left(\frac{1}{k\lambda_{\text{eff}}}\right)\right] . \tag{25}$$

This is in good agreement with the numerical values for $\Phi_1(0, z)$ and illustrates the monotonic decrease of Φ_1 without either oscillation in z or an exponential decay. Using the large argument approximations for the Hankel functions one can show

$$\Phi_1(r \to \infty, z \to \infty) = -\frac{e}{z}\exp\left(-\frac{r}{\lambda_{\text{eff}}}\right)\left[J_0(kr) + \frac{1}{k\lambda_{\text{eff}}}N_0(kr)\right] \tag{26}$$

where N_0 is the Bessel function of the second kind. This helps to explain the good fit of Φ_1 with the product of J_0 with the exponential decay for large z, since $(k\lambda_{\text{eff}})^{-1}$ is small.

As pointed out in the Introduction, a small amount of magnetic shear has been assumed to justify the Landau damping leading to W_I.

Acknowledgments

This work was supported by the U.S. Department of Energy contract #DE-FG05-80ET-53088.

References

1. J.C. Ingraham, R.F. Ellis, J.N. Downing, C.P. Munson, P.G. Weber, and G.A. Wurden, Phys. Fluids B **2**, 143 (1990).

2. V.K. Decyk, G.J. Morales, J.M. Dawson, and H. Abe, 13th European Conf. Contr. Fusion, Pt. II, p. 358, 1986.

3. N. Rostoker and M.N. Rosenbluth, Phys. Fluids **3**, 1 (1960).

4. N. Rostoker and M.N. Rosenbluth, General Atomic Report GAMD-663, Pts. I, II, and III, 1959.

5. T. O'Neil, Phys. Fluids **8**, 2255 (1965).

6. R.C. Davidson, *Methods of Nonlinear Plasma Theory* (Academic Press, New York, 1972) p. 70.

7. A.A. Ware, to be published.

8. N.A. Krall and A.W. Trivelpiece, *Principles of Plasma Physics* (McGraw-Hill, New York, 1973) p. 557.

9. I.S. Gradshteyn and I.M. Ryzhik, *Table of Integrals, Series and Products*, (Academic Press, New York, 1980) p. 721, No. 6.646-1.

10. Wolfram Research, *Mathematica*, (Wolfram Research, Inc., Champaign, Illinois, 1992) Version 2.0.

Figure Captions

1. The numerical solution for $\hat{\Phi}_1$ when $v_0/v_{Te} = 2.5$ is shown as a function of $\hat{r}$ for four values of $\hat{z}$, ($\hat{z} = 0.1$, solid line; $\hat{z} = 1.0$, dot-dashed; $\hat{z} = 10$, dashed and $\hat{z} = 100$ dotted). The values for $\hat{z} = 10$ and 100 have been multiplied by 3 and 30 respectively.

2. The complete normalized potential $\hat{\Phi}$ for the case $v_0/v_{Te} = 2.5$ is shown as a function of $\hat{z}$ for $\hat{r} = 1.0$.

3. Comparison of the numerical solution $\hat{\Phi}_1(\hat{r}, \hat{z} = 10)$ (solid line) and the approximate expression $\exp(b\hat{r})J_0(a\hat{r})/\hat{z}$ (dotted line) for $v_0/v_{Te} = 2.5$.

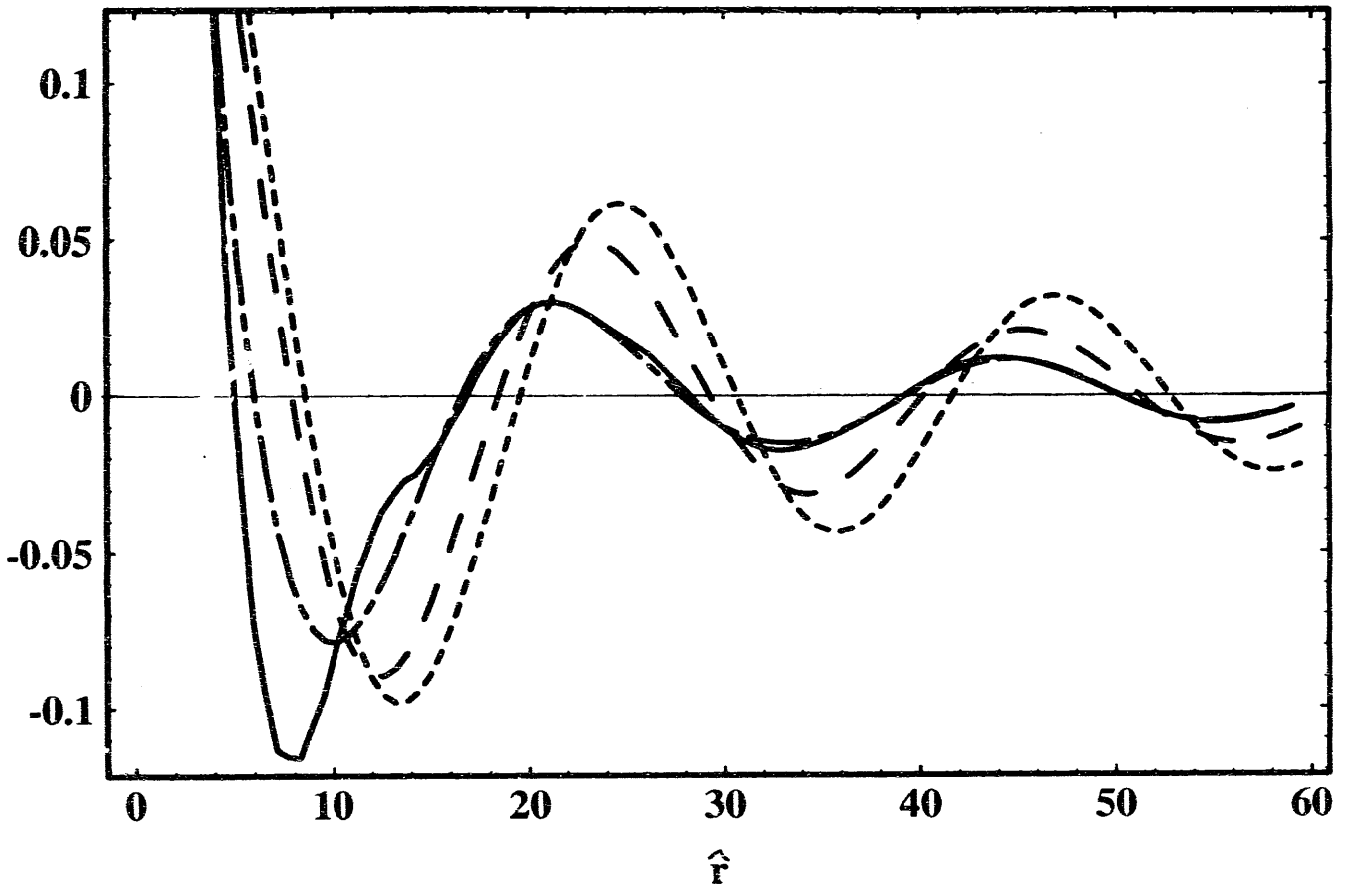

Fig. 1

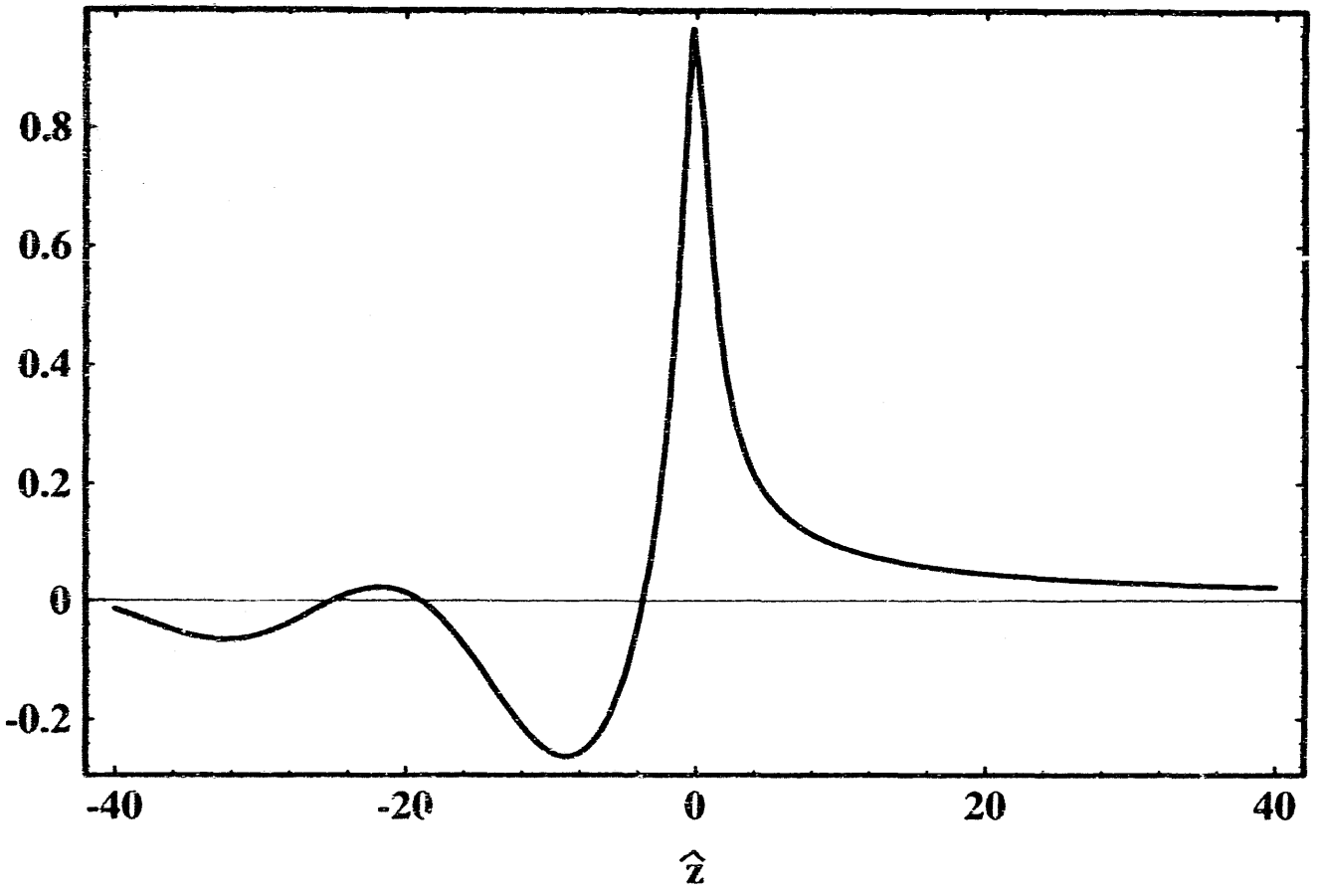

Fig. 2

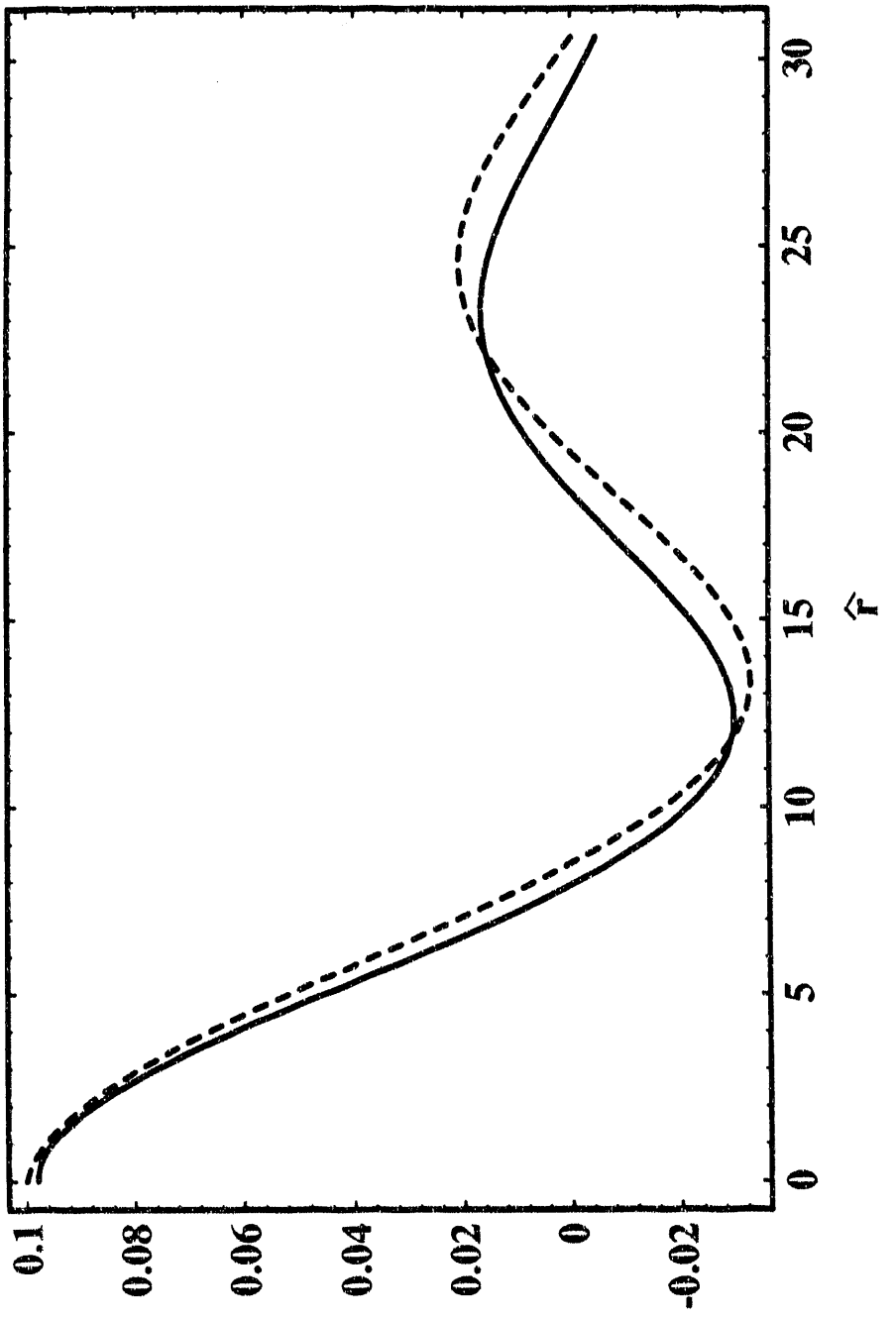

Fig. 3

END

DATE FILMED

10/2/92